

Experimental Evidence for Electron Temperature Fluctuations in the Core Plasma of the W7-AS Stellarator

S. Sattler, H. J. Hartfuss, and W7-AS Team

Max-Planck-Institut für Plasmaphysik, EURATOM, 85748 Garching, Germany

(Received 14 July 1993)

Correlation radiometry has been applied to detect for the first time electron temperature fluctuations in the core of a magnetically confined plasma by means of electron cyclotron emission. Broadband fluctuations are observed in the frequency range up to 150 kHz with levels below 1.4%. Apparent temperature fluctuations due to the finite optical depth are subtracted; the remaining electron temperature fluctuation level is significant. On the basis of reasonable considerations, the results indicate that electron temperature fluctuations can contribute to the anomalous electron heat flux.

PACS numbers: 52.55.Hc

Transport processes in magnetically confined plasmas are not generally described by theoretical models to date. For instance, the electron heat transport coefficients are known for their anomalously high values. Incoherent fluctuations of the electron density as well as of the electron temperature might cause a significant amount of the anomalous heat transport [1,2]. If electron temperature fluctuations are characterized by a similar behavior as density fluctuations [2,3], then wave vectors $k < 1/\rho_s$ ($\approx 10 \text{ cm}^{-1}$ in the relevant region of the W7-AS stellarator; see below), frequencies $f < 1 \text{ MHz}$, and relative amplitudes of about 1% are expected. There is no experimental evidence for the existence of electron temperature fluctuations in the plasma core to date because the requirements on spatial and temporal resolution combined with the sensitivity for small fluctuation amplitudes are not fulfilled by standard core temperature diagnostics [Thomson scattering, soft-x-ray bremsstrahlung spectral analysis, electron cyclotron emission (ECE) radiometry]. In this paper a novel diagnostic technique based on ECE radiometry is presented, which was applied to detect turbulent electron temperature fluctuations in the core of a magnetically confined plasma for the first time. The main emphasis is put on proving the existence of those fluctuations and on the reliability of the method. Details of the fluctuation behavior and its dependence on plasma parameters—although provided by this method—are not the subject of this paper.

To overcome the drawbacks of conventional techniques, correlation radiometry of the ECE is applied. Although standard ECE radiometry has the potential of sufficient spatial and temporal resolution, the required sensitivity for small fluctuation amplitudes is limited by natural fluctuations of the ECE due to the thermal nature of this radiation. The minimum detectable electron temperature fluctuation level $(\tilde{T}_e/T_e)_{\min}$ must exceed the natural fluctuation level at the output of a radiometer [4,5]:

$$\left(\frac{\tilde{T}_e}{T_e}\right)_{\min} > \left(\frac{2B_V}{B_{IF}}\right)^{1/2}. \quad (1)$$

The postdetection bandwidth of the radiometer B_V determines the temporal resolution; the predetection bandwidth B_{IF} determines the spatial resolution along the line of sight. To obtain the required spatial and temporal resolution $B_V = 1 \text{ MHz}$ and $B_{IF} = 500 \text{ MHz}$ is a reasonable choice, resulting in a minimum detectable electron temperature fluctuation level of 6%.

The regime below this value can only be made accessible by applying correlation techniques in order to distinguish between the natural fluctuations of the ECE and the conjectured T_e fluctuations of the emitting plasma volume. Because of the spatial coherence properties of thermal radiation, the natural fluctuations decorrelate if two identical radiometers view the same emitting volume along crossed lines of sight (see Fig. 1) at an angle which exceeds a minimum value, while the temperature fluctuations seen by each radiometer of this “intensity interferometer” [6] remain correlated. Under these conditions cross-correlation analysis then directly gives the rms value of the temperature fluctuations of the common emitting volume. Other decorrelation methods are described in [7–9]. The instrument installed on the W7-AS stellarator [10] ($R = 2 \text{ m}$, $a = 20 \text{ cm}$) consists of two separate absolutely calibrated four-channel heterodyne radiometers designed for measurement of second harmon-

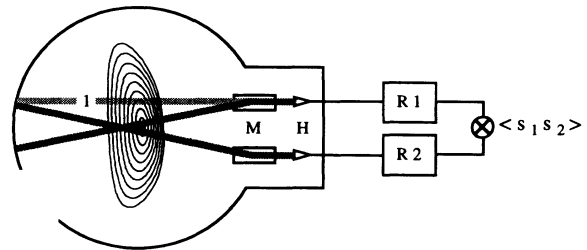


FIG. 1. The intensity interferometer on W7-AS. *M*: elliptical off-axis mirrors, adjustable from outside the vacuum vessel for sight line variation. *H*: corrugated horn antennas. *R*_{1,2}: four-channel heterodyne radiometers. The correlation $\langle s_1 s_2 \rangle$ is calculated numerically. Sight line *l* indicates a position with poloidal separation.

ic X -mode ($E \perp B$) ECE around 145 GHz. The sight lines enclosing an angle of $\approx 20^\circ$ are defined by means of an adjustable Gaussian beam optics [9,11]. The interferometer is sensitive to fluctuation wavelengths which exceed the spatial extent of the emission volume, determined in the radial direction by ECE line broadening effects and the predetection bandwidth B_{IF} ($\Delta R < 1$ cm). Transverse to the sight line it is determined by the width of the Gaussian beams (4 cm full $1/e^2$ width). In magnetic coordinates the k spectrum is integrated up to $k_r = 1.4$ cm^{-1} in the radial direction and up to $k_\perp = 2.3$ cm^{-1} transverse to the beam. Fluctuation frequencies can be measured up to the postdetection bandwidth $B_V = 1$ MHz. The radiometers are sensitive to radiation from the high field side of the W7-AS plasma to avoid interference with relativistically down-shifted emission of suprathermal particles contributing to low field side ECE. The channels cover a radial range with large electron temperature gradients and small electron density gradients ($0.53 < r/a_{\text{separatrix}} < 0.75$). The sensitivity of the intensity interferometer to temperature fluctuations is limited by the statistical error in the correlation function. It is determined by the number of points used for calculating the correlation function and the bandwidth ratio of Eq. (1) [9,12]. With 4×10^6 points, the minimum detectable \tilde{T}_e level is 0.15%. Therefore long stationary phases are necessary and the method has no time resolution. A further increase in sensitivity is obtained by matching post-detection and fluctuation bandwidths with the help of digital filtering. To test the intensity interferometer and to determine the decorrelation angle ($\approx 4^\circ$) a specially developed quasithermal microwave radiation source was used [9].

The maximum of the cross-correlation function at zero delay is a direct measure of the rms value of temperature fluctuations, its decay time a measure of the spectral bandwidth of the fluctuations. Figure 2(a) shows a typical normalized cross-correlation function for the outermost radial position ($r/a = 0.75$). The purely 70 GHz electron cyclotron resonance (ECR) heated plasma is characterized by a peaked electron temperature profile with $T_{e0} = 1.3$ keV and a flat density profile with $n_{e0} = 4 \times 10^{19}$ m^{-3} , as typical for ECRH plasmas on W7-AS [10]. Three structures can be distinguished: (1) a structure with a decay time < 10 μs , (2) a structure with a decay time of ≈ 200 μs , and (3) weak oscillations. The drop of the correlation function below zero is due to a 1 kHz high pass filter, since only the fluctuating signal parts were measured. Figure 2(a) indicates that well distinguishable fluctuation phenomena are present. The high frequency component (1) can be extracted from the others by digital filtering of the correlation function. If low frequency fluctuations and quasicohherent modes are suppressed, a peak remains in the correlation function with a decay time of ≈ 5 μs corresponding to broadband fluctuations with a bandwidth of ≈ 100 kHz. The

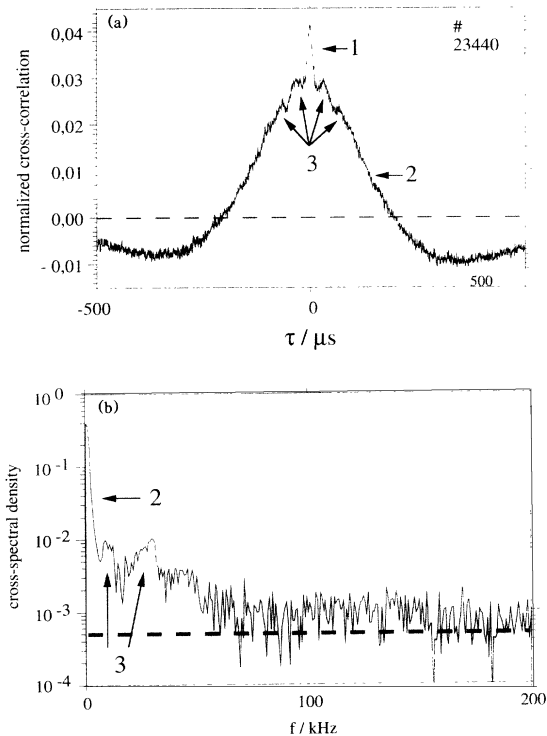


FIG. 2. (a) Typical cross-correlation function calculated from 4×10^6 data points acquired during four shots with 70 GHz ECRH and $T_{e0} = 1.3$ keV, $n_{e0} = 4 \times 10^{19}$ m^{-3} at the center. The scale of the time axis is chosen to identify the annotated structures discussed in the text. (b) Spectral cross-power density of (a), which extends to 1.7 MHz; only the relevant frequency range is plotted. The annotated structures are discussed in the text. The dashed line indicates the noise level.

filtered correlation function provides the rms value of the high frequency fluctuations. The fluctuation power lost by the filtering process is estimated to be lower than 20%. The cross-power spectrum is not as sensitive to broadband fluctuations as the correlation function, since the power is spread over a wide spectral range. However, low frequency fluctuations with $f \leq 5$ kHz [Fig. 2(b) 2, corresponding to 2 in Fig. 2(a)] and two quasicohherent modes with mean frequencies of $f \approx 10$ kHz and $f \approx 28$ kHz [Fig. 2(b) 3, corresponding to 3 in Fig. 2(a)] can be identified. To obtain spectral information on the high frequency component of the fluctuations even more data have to be averaged. In all discharges examined, fluctuations appear in two frequency ranges: $f < 15$ kHz and $f < 150$ kHz. In some cases they are not well distinguishable.

The quantity derived from the cross-correlation function is the rms value of radiation temperature fluctuations \tilde{T}_R . The radiation temperature T_R approaches the electron temperature T_e only if the optical depth τ is sufficiently large:

$$T_R = T_e(1 - e^{-\tau}) \quad \text{where } \tau \sim n_e T_e. \quad (2)$$

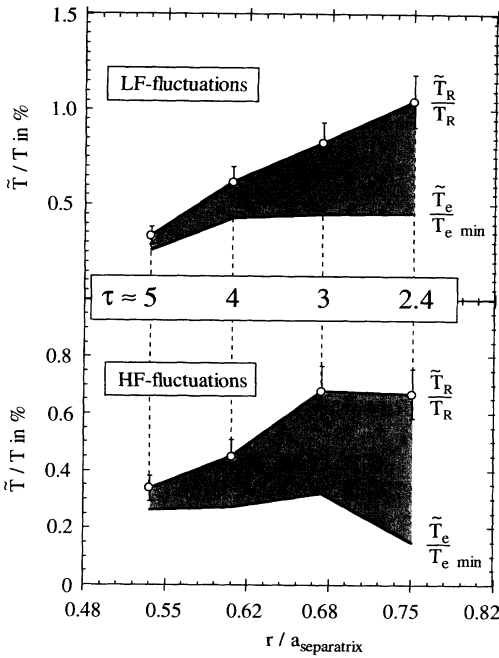


FIG. 3. Radial fluctuation profiles for low frequency fluctuations (LF) and high frequency fluctuations (HF). Open circles give the measured radiation temperature fluctuation level with error bars. The solid line indicates the lower limit for the true electron temperature fluctuation level, if 2% density fluctuations as an upper limit are assumed. τ is the optical depth as calculated from density and temperature profiles.

The radial profile of the fluctuation level \tilde{T}_R/T_R is given in Fig. 3 as a typical result. The error bars are about 12% of the measured \tilde{T}_R/T_R given by the statistical error in the correlation function and the calibration error. To interpret radiation temperature fluctuations as electron temperature fluctuations, the possible influence of density and electron temperature fluctuations must be discussed. Any density fluctuation causes a fluctuation of the optical depth and therefore radiation temperature fluctuations even with constant T_e . In addition, any electron temperature fluctuation \tilde{T}_e produces a \tilde{T}_R level higher than the true \tilde{T}_e level by the same mechanism. Significant influences are expected only if the optical depth is low ($\tau < 5$). The radiation temperature fluctuation level can be calculated by differentiating Eq. (2):

$$\frac{d\tilde{T}_R}{\tilde{T}_R} \approx \frac{\tilde{T}_R}{T_R} = (1+a) \frac{\tilde{T}_e}{T_e} + a \frac{\tilde{n}_e}{n_e} \quad \text{with } a = \frac{\langle \tau \rangle e^{-\langle \tau \rangle}}{1 - e^{-\langle \tau \rangle}}, \quad (3)$$

where $\langle \tau \rangle$ is the mean optical depth. Equation (3) is used to estimate the true \tilde{T}_e/T_e level. The \tilde{T}_R/T_R level is measured and τ is calculated from T_e and n_e profiles to be between 2.4 and 5 (Fig. 3). The density fluctuation level as measured by reflectometry decreases monotonically from the edge, reaching $\tilde{n}_e/n_e = 2\% - 3\%$ at $r/a = 0.79$.

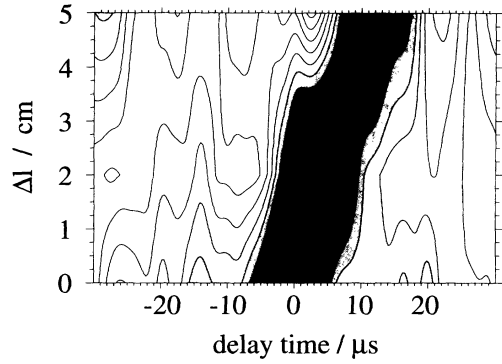


FIG. 4. Contour plot of normalized cross-correlation functions for three different poloidal distances ($\Delta l = 0, 2,$ and 5 cm in magnetic coordinates). The contours are calculated by an interpolation routine; they are shaded for levels above 0.1. The darkest region corresponds to levels between 0.9 and 1.0. The width of the correlation function is $\approx 5 \mu\text{s}$; the time shift of the correlation maximum for $\Delta l = 5$ cm is $\approx 11 \mu\text{s}$.

For $0.53 < r/a < 0.75$, accessible to the intensity interferometer, \tilde{n}_e/n_e is assumed to be a constant 2%. This is an overestimate, since the density fluctuation level is expected to decrease further with decreasing density gradient towards the plasma center. In addition, the reflectometer is sensitive to higher k values ($k < 4 \text{ cm}^{-1}$) than the intensity interferometer and hence only a part of the \tilde{n}_e level affects the interferometer measurements. Therefore the true \tilde{T}_e/T_e level calculated by means of Eq. (3) gives a lower limit (Fig. 3). In all discharges examined, the low frequency fluctuations were found with levels between 0.08% and 1.4% and the high frequency fluctuations were found with levels between 0.2% and 0.8%. The lowest levels correspond to the innermost radial positions. In some shots, the high frequency fluctuations drop at the innermost positions below the sensitivity level of the instrument. The lower limits for electron temperature fluctuations are 80% (30%) of the measured radiation temperature fluctuations for the innermost (outermost) radial positions as given by finite optical depth corrections. The remaining levels are above the error bars in all cases.

The high frequency fluctuations show a poloidal velocity, which can be measured by a different correlation technique; however, this method is not suitable for determining the absolute fluctuation level: If the sight lines are adjusted as marked by 1 in Fig. 1, a poloidal distance is introduced between the emission volumes of the sight lines. The volumes are still located close to a common flux surface. As a result the correlation maxima of the high frequency fluctuations are shifted in time (Fig. 4). The 5 cm distance gives rise to a 11 μs shift in time from which a poloidal velocity of 4.5 km/s can be derived. The direction of propagation is in the electron diamagnetic drift direction. The electron diamagnetic drift velocity at the same radial position is ≈ 3.5 km/s. Since the low

frequency fluctuations do not show a significant poloidal velocity, the separation into low and high frequency components is justified. The estimate of correlation lengths from this type of measurement needs further investigation, because the \tilde{T}_e levels are unknown in this type of experiment.

The influence of temperature fluctuations on transport can be estimated, if assumptions on fluctuations of the poloidal electric field \tilde{E}_θ and the phase between \tilde{E}_θ and \tilde{T}_e are made. The part of the electrostatic fluctuation driven electron heat flux containing \tilde{T}_e is given by [2]

$$Q_{\tilde{T}_e} = \frac{3}{2} k_B n_e \langle \tilde{T}_e \tilde{E}_\theta \rangle / B_\phi$$

$$\approx \frac{3}{2} \frac{\Delta k_\theta n_e (k_B T_e)^2}{e B_\phi} \frac{e \tilde{\phi}}{k_B T_e} \frac{\tilde{T}_e}{T_e}. \quad (4)$$

The ensemble average is replaced by the rms values of the fluctuations assuming the phase relationship for maximum transport. A $e\tilde{\phi}/k_B T_e$ level of 3% is assumed, which is slightly above \tilde{n}_e/n_e as predicted by theoretical models (e.g., [13]). The width of the k spectrum is unknown, only the detectable range of about $\Delta k \approx 2 \text{ cm}^{-1}$ is considered. The \tilde{T}_e/T_e level for the innermost position of the example above is 0.38% for both types of broadband fluctuations added as statistically independent. The definition of an equivalent electron heat diffusivity, $\chi_e = -Q_{\tilde{T}_e}/k_B n_e \nabla T_e$, yields $\chi_e = 0.4 \text{ m}^2/\text{s}$. It indicates that electron temperature fluctuations, even at such low levels, might significantly contribute to the measured electron

heat transport dominated diffusivity on W7-AS, where χ_e is typically $1 \text{ m}^2/\text{s}$ for the plasmas considered [10].

This work is part of a Ph.D. thesis at the Heinrich-Heine-Universität Düsseldorf, Germany.

-
- [1] P. C. Liewer, J. M. McChesney, S. J. Zweben, and R. W. Gould, *Phys. Fluids* **29**, 309 (1986).
 - [2] A. J. Wootton, B. A. Carreras, H. Matsumoto, K. McGuire, W. A. Peebles, Ch. P. Ritz, P. W. Terry, and S. J. Zweben, *Phys. Fluids B* **2**, 2879–2903 (1990).
 - [3] P. C. Liewer, *Nucl. Fusion* **25**, 543–621 (1985).
 - [4] G. Bekefi, *Radiation Processes in Plasmas* (Wiley, New York, 1966).
 - [5] A. Cavallo and R. Cano, *Plasma Phys. Controlled Fusion* **23**, 61–65 (1981).
 - [6] R. Hanbury-Brown and R. Q. Twiss, *Philos. Mag.* **45**, 663–682 (1954).
 - [7] G. Cima, *Rev. Sci. Instrum.* **63**, 4630–4632 (1992).
 - [8] M. Kwon, R. F. Gandy, C. E. Thomas, and W. K. Lim, *Rev. Sci. Instrum.* **63**, 4633–4635 (1992).
 - [9] S. Sattler and H. J. Hartfuss, *Plasma Phys. Controlled Fusion* **35**, 1285–1306 (1993).
 - [10] H. Ringler *et al.*, *Plasma Phys. Controlled Fusion* **32**, 933–948 (1990).
 - [11] H. J. Hartfuss and M. Tutter, *Rev. Sci. Instrum.* **56**, 1703–1705 (1985).
 - [12] J. S. Bendat and A. G. Piersol, *Measurement and Analysis of Random Data* (Wiley, New York, 1966).
 - [13] B. D. Scott, *Phys. Fluids B* **4**, 2468 (1992).

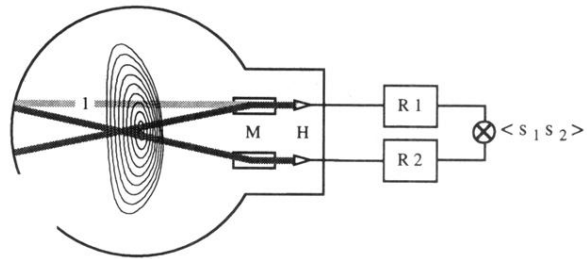


FIG. 1. The intensity interferometer on W7-AS. *M*: elliptical off-axis mirrors, adjustable from outside the vacuum vessel for sight line variation. *H*: corrugated horn antennas. *R*_{1,2}: four-channel heterodyne radiometers. The correlation $\langle s_1 s_2 \rangle$ is calculated numerically. Sight line 1 indicates a position with poloidal separation.

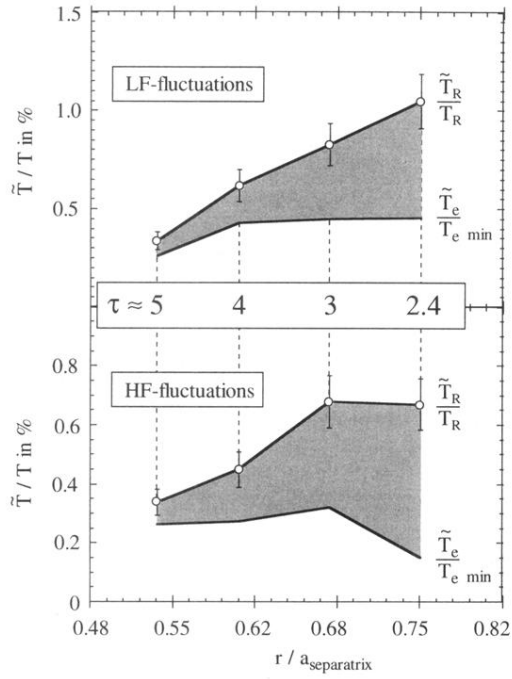


FIG. 3. Radial fluctuation profiles for low frequency fluctuations (LF) and high frequency fluctuations (HF). Open circles give the measured radiation temperature fluctuation level with error bars. The solid line indicates the lower limit for the true electron temperature fluctuation level, if 2% density fluctuations as an upper limit are assumed. τ is the optical depth as calculated from density and temperature profiles.

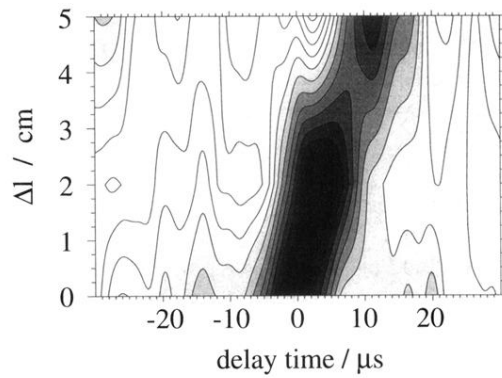


FIG. 4. Contour plot of normalized cross-correlation functions for three different poloidal distances ($\Delta l = 0, 2,$ and 5 cm in magnetic coordinates). The contours are calculated by an interpolation routine; they are shaded for levels above 0.1 . The darkest region corresponds to levels between 0.9 and 1.0 . The width of the correlation function is $\approx 5 \mu\text{s}$; the time shift of the correlation maximum for $\Delta l = 5$ cm is $\approx 11 \mu\text{s}$.